Residual immunity and seasonality of an epidemic

Siyu Chen[1*]

[1]High Meadows Environmental Institute, Princeton University, Princeton, NJ 08544
[*]Corresponding author: Siyu Chen, siyu.chen@princeton.edu

Abstract

We present a dynamical model of the onset and severity of cyclical epidemic disease taking account not only of seasonal boosts during the infectious season, but also of residual immunity remaining from one season to the next. After studying the mathematical properties of the model and the role of its parameters, we focus on the effect of titers remaining after one season on the timing and severity of the onset of the next season's epidemic. Suppressing the epidemic for one season, or witnessing a strong surge for one season, both have lasting effects for a number of successive seasons.

1 Introduction

We propose a minimal model of the immunity to a seasonal epidemic disease, exemplified by influenza [1], taking account not only of exposure-induced boosts during the infectious season, but also of the waning of residual immunity remaining from one season to the next. An exclusive focus on antibody levels contrasts with other models of the progress of an epidemic, involving multiple population sectors, and many parameters interacting with the waning process. With our minimal model, purely analytic closed-form solutions combining the separate effects of individual parameters can be derived.

Classical epidemiological models focus on the individuals in a population, whether they are susceptible to infection, exposed to the pathogen, symptomatic, hospitalized, in ICU, recovered or deceased. Populations are subdivided by age, sex, socioeconomic level and geographical location. Epidemic models calculate the number of individuals with different statuses and account for their movements from one subgroup to another. Departing from these individual-based models, a direct accounting for the population average titre of antibodies

against the pathogen implicated in the epidemic should track the overall progression of the epidemic, avoiding the numerous parameters required in compartmental models.

Our model features an exponential waning process during and between annual seasons, imposed on the temporal distribution of infections or exposures over a season. The latter distribution, especially the timing of peak infectivity, interacting with the waning function, is all that is necessary to reproduce, in mathematically closed form, the mechanical cycle of boosting and waning immunity characteristic of recurrent seasonal infectious disease. Distinct from epidemiological models predicting numbers of individuals moving between infectivity categories, our result enables us to directly confront the parameters of waning and the infectivity distribution. Our invocation of an exponential decay of immunity has many antecedents in the literature, e.g., [2, 3, 4]. In addition, although studies such as [5] have empirically derived mathematical forms for the residual immunity from one season to the next, these do not model the process of waning.

We can naturally iterate the cyclical boost-and-wane process to simulate immunity trajectories over many years and thus to quantify the relationship between residual immunity and the time elapsed between annual infectivity peaks, namely a relation between end-of-season titre and the length of the interval between annual infectivity peaks.

Determining the onset of epidemic outbreak, whether of an emerging, newly recognized, virulent pathogen [6] or of a recurrent seasonal infection [7, 8, 9], is a vexing problem both for epidemiological research and for population health planning. This has been stressed for a variety of recurrent viral epidemics worldwide [10, 11, 12].

The onset and severity of an epidemic are largely unpredictable. But there was widespread prediction that the lowering of antibody levels against influenza [13] and RSV [14] as a side-effect of non-pharmaceutical interventions during the Covid-19 pandemic (masking, testing, lockdown, isolation,...) would lead to early onset and increased severity of epidemics of these diseases after the pandemic. And this prediction was validated in subsequent seasons.

Our model incorporates a probabilistic determination of peak infectivity, is naturally adaptable to our goal through the linking of the peak probabilities to the pre-season titres. And the severity, or amplitude, which in our model is linearly predictive of post-season titres, can be linked in the same way to the pre-existing titres.

Many other factors may enter into the timing of the induction of an infectious season, such as climate, demographic changes, antigenic shift in the pathogen, changes in transmission patterns [10], and others. Nevertheless low residual titre levels remain a likely driver of early onset and peak times and severity.

2 The model

2.1 An infectious cycle for a single season

The average titre of a population will increase because of new exposures but decrease due to antiody waning, as sketched in Figure 1. Our model contains a minimum of elements, namely a probability distribution $f(t)$ reflecting the force of infection, e.g., the rate at which susceptible individuals in a population acquire an infectious disease, and an antibody decay rate ω.

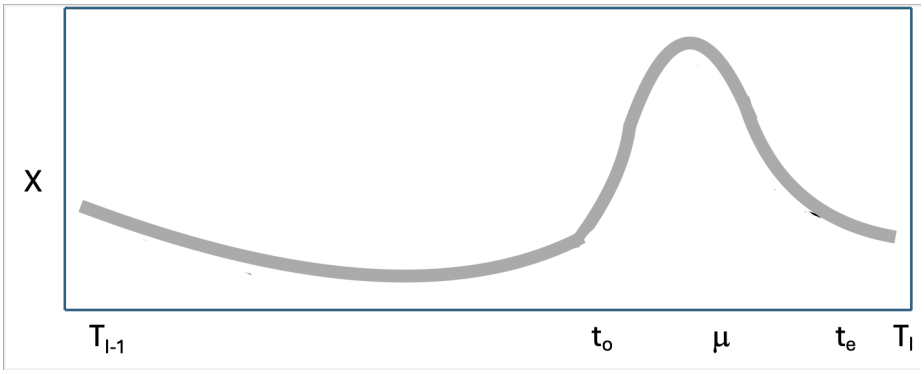

Figure 1: Concept of basic model.

We exemplify $f(t)$ with a raised cosine function, parametrized as:

$$f_\mu(t) = \begin{cases} \frac{a}{2\pi}(1+\cos a(t-\mu)), & \text{if } t \in [t_o, t_e] \\ 0, & \text{otherwise} \end{cases} \tag{1}$$

where an infectious season starts from date $t_o = \mu - \frac{\pi}{a}$ and ends on date $t_e = \mu + \frac{\pi}{a}$, where μ is the peak month of the severity of the current infectious season. Then the change of antibody titres between any time point T_{i-1}, before the i-th season, and T_i, after the i-th season, for all $i \geq 1$, can be calculated by the relation:

$$X_{T_i} = X_{T_{i-1}} e^{-\omega(T_i - T_{i-1})} + \int_{T_{i-1}}^{T_i} \beta_i f_\mu(t) e^{-\omega(T_i - t)} dt, \tag{2}$$

where β_i is the amplitude or severity of the infectious season.

From the definition in (1), Equation (2) becomes

$$X_{T_i} = X_{T_{i-1}} e^{-\omega(T_i - T_{i-1})} + \beta_i e^{-\omega T_i} \int_{t_o}^{t_e} \frac{a}{2\pi}(1+\cos a(t-\mu)) e^{\omega t} dt, \tag{3}$$

Then, using the definition of t_o and t_e, the integral in (3) has closed form

$$e^{\mu w}\frac{\sinh(\pi\theta)}{\pi\theta(1+\theta^2)}, \tag{4}$$

where $\theta = \frac{\omega}{a}$. Equation (3) can then be rewritten

$$X_{T_i} = X_{T_{i-1}}e^{-\omega(T_i-T_{i-1})} + \beta_i e^{-\omega(T_i-\mu)}\frac{\sinh(\pi\theta)}{\pi\theta(1+\theta^2)}. \tag{5}$$

2.2 A fixed point of an iterated model for multiple seasons

Using a given inital titre X_{T_0} to calculate X_{T_1} by Equations (2) or (5), and using the calculated X_{T_1} to calculate X_{T_2}, and continuing the same way for $X_{T_3}, X_{T_4}, \cdots$, we have defined a discrete dynamic system, at times $T_0 < T_1 < \cdots$. We can assume $T_i - T_{i-1} > \Delta > 0$, for some Δ and for all $i \geq 1$. Given two initial titres X_{T_0} and Y_{T_0}, we can see that

$$\|X_{T_i} - Y_{T_i}\| = \|X_{T_{i-1}} - Y_{T_{i-1}}\|e^{-\omega(T_i-T_{i-1})} \tag{6}$$

since the integral is constant, for $i = 1, 2, \cdots$. Now $e^{-\omega\Delta} < 1$, so this process is contractive, with Lipschitz constant $e^{-\omega\Delta}$.

It has a fixed point

$$\frac{\beta e^{-\omega\delta}\frac{\sinh(\pi\theta)}{\pi\theta(1+\theta^2)}}{1-e^{-\omega\Delta}}, \tag{7}$$

in the simplest case, where $\beta = \beta_i$, $\delta = T_i - \mu$ and $\Delta = T_i - T_{i-1}$ for all i.

For example, we may examine the default parameters $\beta = 1, \omega = \frac{1}{24}, \mu = 12, a^{-1} = \frac{2}{\pi}, \Delta = T_i - T_{i-1} = 12, \delta = T_i - \mu = 3$, to determine the fixed point $X = 2.24$. This may be compared to the numerical results in Figure 2 tracking two trajectories of the model over 20 seasons.

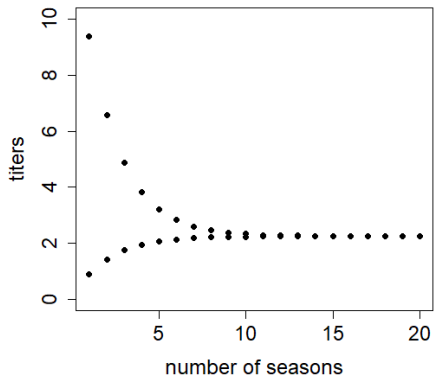

Figure 2: Convergence to one fixed point from two initial points.

2.3 The role of the parameters

The rate of resistance waning warrants closer modeling than the linear decline over a few months or a year (as in [15]). Here we consider an exponential decay of immunity, expressed in terms of abstract units of antibody titre per unit time, with parameter ω.

Figure 3(a) shows the effect of this parameter. For very high waning rates, the output titre is decreased, while lower values of ω result in X_{T_I} conserving much of the input titre and even surpassing it.

As for the parameter representing seasonality, namely the peak infectivity date μ, an early or late season will increase or decrease the time until T_i, as seen in Figure 3(b), increasing or decreasing waning time, respectively. This effect follows a largely linear response, and is substantial.

We note that the model parameters μ, t_o, t_e and β are relatively accessible to direct observation through public health statistics, e.g.,[16],[17], but ω can only be inferred indirectly.

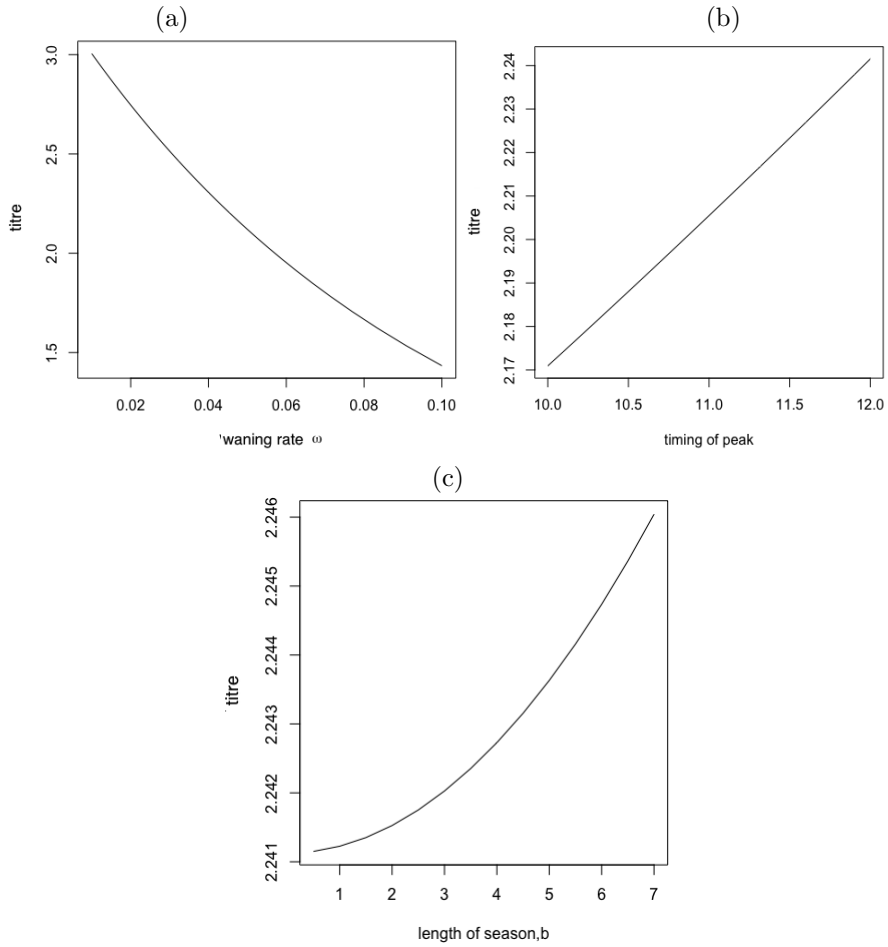

Figure 3: (a) Effect of the waning parameter ω on X_{T_I}. (b) Effect of early or delayed season (c) Effect of duration of season.

3 Long-term trends

3.1 Random peaks

As a benchmark experiment, we concatenated successive instances of the model of a single cycle described in Section 2 to carry out a simulation of 20 recurrent infectious seasons interspersed with quiescent periods for the rest of each cycle (i.e., year).

Initialized with a random titre at date T_1 corresponding to the end of a typical infectious period, the peak infection date m was chosen from a uniform prob-

ability over a wide range, September (month 9) to April (month 16), and the first iteration was performed with T_2 set to be $m + \frac{\pi}{a}$, with output X_{T_2}.

The output X_{T_2} at time T_2 from the first cycle, is then used as the starting titre X_{T_3} at time T_3 of the second cycle. The peak of infections is again randomly chosen from September to April.

This calculation is repeated for the third and subsequent cycles. Figure 4(a) shows five typical trajectories of X_T over the 20-year span. The randomness in the choice of peaks prevented the process from simply degenerating into a fixed point limit cycle, but maintained a stable pattern of random variation indefinitely.

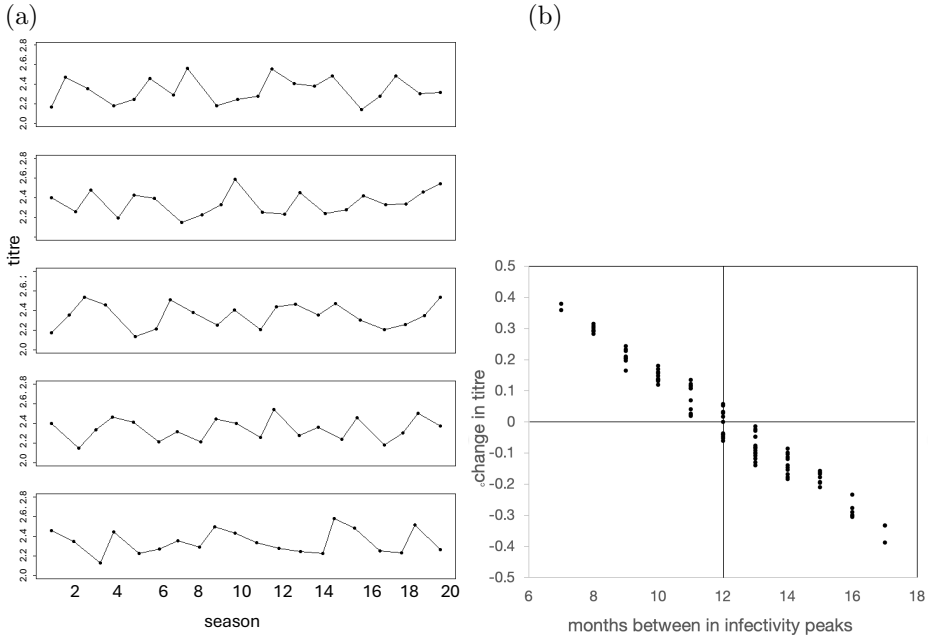

Figure 4: (a) Sample trajectories of 20 seasons produced by iterating the model, five replicates. (b) Association of titre change with length of inter-season times.

How can we characterize this pattern formally? There is a contractive model as in Equation (2) corresponding to each value of μ. But as the model is changing with most iterations of the process, the approach to the fixed point(s) is disrupted at each step.

There are r different values of μ, corresponding to the months from September to April ($r = 8$). If we imposed the unrealistic conditions that the process repeated indefinitely along a fixed trajectory among all the r values of μ then there would exist a fixed orbit of r points, to which the successive titres in the

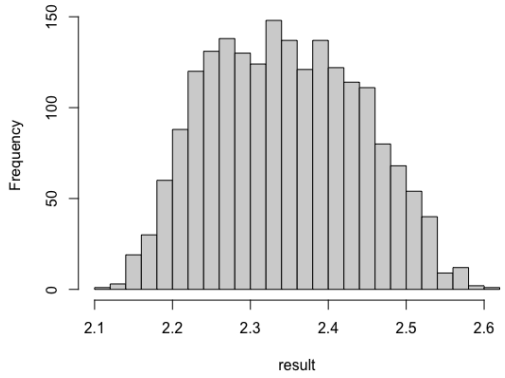

Figure 5: Longterm distribution of titers of the iterated model.

trajectory would converge over time. But once we allow complete randomness in the successive values of μ among the r possibilities, as is necessary in our epidemic model, then no such fixed orbit exists. Instead, we can only say that the distribution of titre values converges to a fixed distribution with support $[s_1, s_r]$, where s_1 and s_r represent the minimum and maximum fixed points of the r models, as in Figure 5.

We plotted the change in titre $\Delta_X = X_{T_i} - X_{T_{i-1}}$ as a function of $\Delta_\mu = \mu_i - \mu_{i-1}$, the shift in peak infections between the $i-1$-st and i-th cycle. The results in Figure 4(b) show a tight linear relation between the two quantities. The slope is -0.71 titre units/12 months differential, or 0.059 units/month. This compares to $\log \omega = 0.042$/month.

3.2 Training for seasonality

The negative correlation between the change of output titre and the time elapsed between successive peaks in Figure 4(b) must be seen as a function only of the waning time between two seasons, since there is no mechanism within the model to affect one year's peak μ as a direct function of the previous year's output titre $X_{T_{I-1}}$. Such a mechanism, however, is widely thought to be of importance to recurrent epidemics.

To train the model as a predictor of seasonality, we made use of the results of the experiment described in Section 3.1. Based on each year's $X_{T_{i-1}}$, a random choice of next year's peak month μ_i was effected. This choice involved two steps: The first was the deterministic choice of one of four bins, $B_1, \cdots, B_4$, with B_1 containing the highest values of $X_{T_{i-1}}$, and B_4 containing the lowest

values of $X_{T_{i-1}}$. The second step was a uniform random choice among THREE consecutive months. The months in each bin overlapped those in the adjacent bins, with B_1 containing December through March, B_2 containing November through February, B_3 containing October through January and B_4 containing September through December.

A 200-season experiment could then be initiated by a random choice of X_{T_0}. There was no further addition of noise or other intervention over the length of the experiment. Because setting a new peak month determines a different fixed point for X_{T_i}, each iteration of the model gives an different output from the previous season's.

Figure 6(a) shows one aspect of the outcome, comparing the titres of each pair of successive seasons. The extent of the scatter is largely the effect of the large overlapping bins from which to choose the peak month.

3.3 Using the model to predict the peak of the next epidemic season

We regress the peak date chosen against the input titre for the data in Section 3.2. This produces the following result:

$$\text{peak month} = 2.815 \times \text{titre} - 0.068 + \epsilon \tag{8}$$

where the normal error ϵ has a standard deviation of 0.45.

This result can then be used as a predictive tool. Given an end-of-season titre X_{T_i}, Equation (8) can predict the likely peak month and the shape of the titre distribution during the season. For example, using the parameters in Figure 6(b), an end-of-season titre of 4.7 predicts an early January peak, but distributed with a standard deviation of about two weeks.

3.4 Lasting effects of a missing season

The dramatically diminished influenza epidemic resulting from the Covid pandemic-inspired non-pharmaceutical interventions in 2020-22 was followed by an early onset and severe influenza season in 2022-2023. This was predictable [13], given the lack of newly acquired immunity during the pandemic.

From the modeling viewpoint, this aspect of the seasonality-titre relationship, can be expressed by simply introducing a single missing (zero-amplitude) season, and following the trajectory of the process in subsequent years.

To accomplish this we started with the model in Section 3.2. In one experiment over fifty years, we introduced an "$\beta = 0$" year every eighth year. In a second experiment we introduced an "$\beta = 0$" year every four years. We

(a)

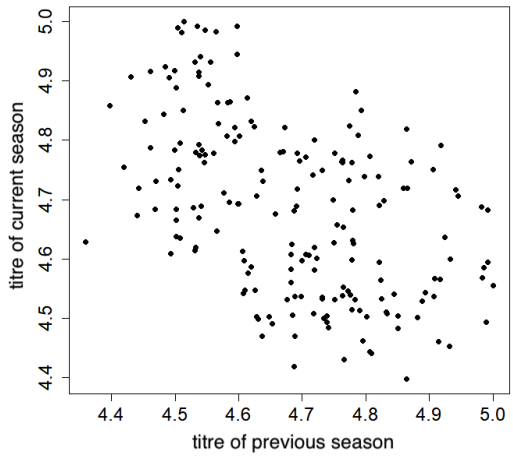

(b)

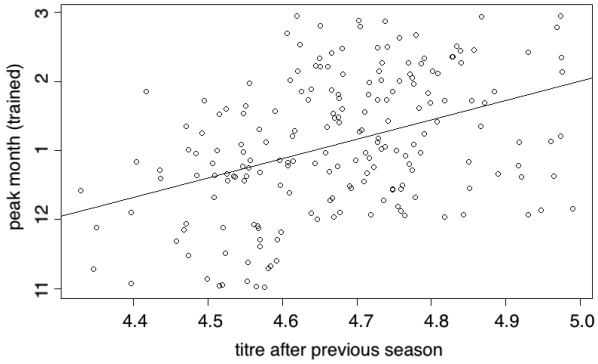

Figure 6: (a) Effect of training on titres of successive seasons. (b) Effect of training on choice of peak month, with regression line.

then compared the trajectory from these two experiments with that from the original, unmodified, experiment, where $\beta = 1$ for every season.

The results in Figure 7 show that for the experiment with an 8-year cycle, the effect of a reduced titre persisted over five to seven years, before catching up to the sequence of unmodified seasons. On the other hand, with a four-year cycle, the output titre never quite caught up .

Figure 7(a) summarizes the differences among these trajectories.

Figure 7(b) shows how the titres of the two missing-seasons trajectories gradually increase towards the unmodified (no missing seasons) pattern.

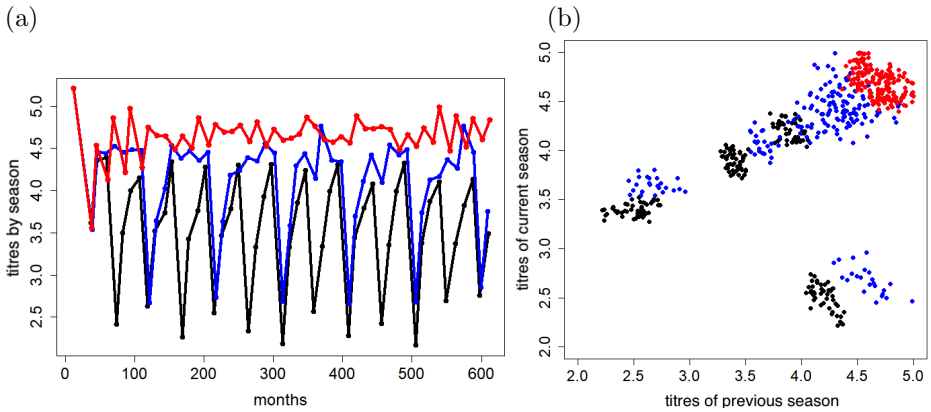

Figure 7: (a) End-of-season titre trajectories with an 8-year pattern of a missing season (blue), a 4-year pattern (black) and with no missing seasons. (red). (b) Change of titre from one season to the next. Displaced clusters represent the immediate effect of the missing boost.

3.5 Lasting effects of a severe season

In a way analogous to the method in the Section 3.4, we can model the after-effects of a severe season, by setting $\beta = 2$ for one season out of four, or one season out of eight, while $\beta = 1$ for all the remaining seasons. The results of this

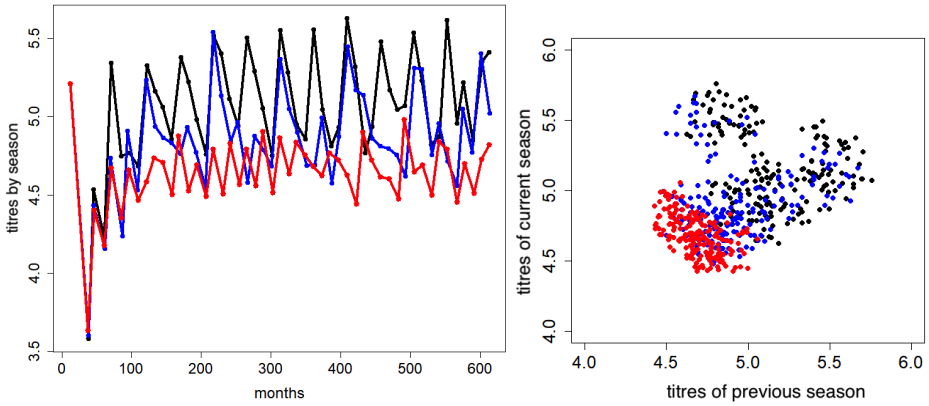

Figure 8: (a) End-of-season titre trajectories with an 8-year pattern of severe seasons (blue), a 4-year pattern (black) and with no severe seasons (red). (b) Change of titre from one season to the next. Displaced clusters represent the immediate effect of the amplified boost.

experiment mirror those of the "missing season" experiment, but in the opposite direction. Figure 8 (a) shows how the titres in the 8-year pattern eventually

settle down to rates comparable to the unmodified sequence, while the 4-year pattern retains elevated titres throughout.

Figure 8(b) shows how the titres of the two missing-seasons trajectories gradually decrease towards the unmodified (no severe seasons) pattern.

4 Further work

4.1 Introducing age structure and other compartments

We can model the differential dynamics of, for example, adults and children. This would require two models with identical parameters, but which differ only in the random choice of μ. To model that children are often drivers of epidemics for certain infectious diseases, the choice of μ for adults would depend on preceding choice of μ for children. An early onset for children would trigger a early onset for adults soon afterwards. Thus if $X^{(A)}$ represents the model for adults and $X^{(C)}$ represents the model for children, we assume $X^{(A)}_{T_i} = X^{(C)}_{T_i}$, and based on that titre, we choose μ^A_i and μ^C_i independently and randomly from among the months 9-16 (September to April). If $\mu^C_i - \mu^A_i > 1$, then we reset $\mu^A_i = \mu^C_i - 1$. At time T_i, we add $W(A)X^{(A)}_{T_i} + W(C)X^{(C)}_{T_i}$ to produce the total population titre X_{T_i}, where W is the proportion of the population represented by adults and children.

The effect of this choice is model the response to an early outbreak among children. This leads to an early outbreak among adults.

In contrast to the movement of individuals in classical compartmental models, our model does not involve the transfer of titres between the two age groups. The effect of one compartment affecting another is modeled in the choice of μ and/or β in one compartment depending on the recent state of the process in a "neighbouring" compartment, such as age group, spatial proximity, health workers versus general public or interacting occupational groups.

The overall titre dynamics of the whole population is calculated as the sum of the submodel titres, weighted by the pertinent population numbers or porportions W.

4.2 Endemicity and random emergence of epidemics

Introducing a small, but variable titre maintained in the population between epidemics, in the spirit of Kermack-McKendrick, would allow us to apply a threshold for the the re-emergence of epidemic. This would replace the seasonality embodied in the annual choice of μ.

5 Discussion and conclusions

The core of our experimental model takes into account only titre increases during a few months-long season of an infectious disease with fixed infectivity peak μ, plus a continuous process of waning, expressed by a negative exponential with parameter ω. These two processes can reproduce the cycle of boosting and waning characteristic of recurrent seasonal infectious disease.

Iterating this model, however, is not suitable for generating long term trajectories of an epidemic. Mathematically, it is a contractive process that would quickly converge towards a sequence of identical seasons.

Replacing the assumption of fixed peak times with a random choice among several months, however, nullified the contractive tendency, so that we could explore the variation in titre as a function of the peak location parameter μ. This revealed a strong association between shift of peak month and change of titre at the end of the season.

Introducing an element of causality into this association, we trained the model so that a lower titre in the previous year would lead to a early onset in of the epidemic in the current year, via a slight bias in the random selection of the peak month, while a larger titre would delay the season.

The pattern that emerged from this training then allowed us to establish a prediction rule so that from the titre at the end of one season, we can predict the timing of the next one, in terms of a probability distribution of the timing of the peak month.

Inspired by the dramatic drop of infections by non-covid respiratory viruses like influenza and RSV in the 2021-2022 season, followed by a strong resurgence in the following year, we adapted our model by setting the amplitude (severity) parameter A to zero for one year out of four or one year out of eight and observed how such perturbations affected subsequent years.

These experiments showed that after each of the "missing" years, the trajectories of the post-season titres inevitably recovered towards the usual pattern, largely in the case of the four-year cycle, but completely in the case of the eight-year cycle.

To study the effects of a year with increased severity, we set the parameter β to 2.0 for one year out of four or one year out of eight and observed how such perturbations affected subsequent years, similar to the experiment with missing years.

These experiments showed that after each of the severe years, the trajectories of the post-season titres inevitably reverted towards the usual pattern, largely in the case of the four-year cycle, but completely in the case of the eight-year cycle.

This timing is of course dependent on our choice of parameters and protocols:

ω, β, the training protocol, and predicting the distribution of μ. Nevertheless, it illustrates the kind of investigation possible with our titre-based modelling.

Our discussion has been phrased in terms of antibody titres, but the generality of our model means that it is not specifically limited to any specific aspect of the infectious disease season or yearly cycle, such as exposures, infections, symptoms, seroprevalence or antibody levels, as long as the annual boost can be represented by a distribution.

In this work, we have not assumed anything about viral strains. Apparent waning over several seasons may reflect mutational drift or selection in the antigen, rather than immunological processes per se. This does not distract from the pertinence of our model as a basis for analyzing the cyclical behaviour of boosting and waning.

References

[1] Brauer F, Castillo-Chavez C, Feng Z, Brauer F, Castillo-Chavez C, Feng Z. Models for Influenza. In: Mathematical models in epidemiology. New York: Springer; 2019: 311-50.

[2] Antia A, Ahmed H, Handel A, Carlson NE, Amanna IJ, Antia R, Slifka M. Heterogeneity and longevity of antibody memory to viruses and vaccines. PLoS biology. 2018 Aug 10;16(8):e2006601.

[3] Vattiato G, Lustig A, Maclaren OJ, Plank MJ. Modelling the dynamics of infection, waning of immunity and re-infection with the Omicron variant of SARS-CoV-2 in Aotearoa New Zealand. Epidemics. 2022 Dec 1;41:100657.

[4] El Khalifi M, Britton T. El Khalifi M, Britton T. Extending susceptible-infectious-recovered-susceptible epidemics to allow for gradual waning of immunity. Journal of the Royal Society Interface. 2023 Sep 13;20(206): 20230042.

[5] Zhao X, Ning Y, Chen MI, Cook AR. Individual and population trajectories of influenza antibody titres over multiple seasons in a tropical country. American Journal of Epidemiology. 2018 Jan 1;187(1):135-43.

[6] Chen S, Flegg JA, White LJ, Aguas R. Levels of SARS-CoV-2 population exposure are considerably higher than suggested by seroprevalence surveys. PLoS computational biology. 2021 Sep 20;17(9):e1009436.

[7] C.J. Rhodes, T.D. Hollingsworth, Variational data assimilation with epidemic models, Journal of Theoretical Biology, Volume 258, Issue 4, 2009.

[8] Giorgia Vattiato, Audrey Lustig, Oliver J. Maclaren, Michael J. Plank, Modelling the dynamics of infection, waning of immunity and re-infection with the Omicron variant of SARS-CoV-2 in Aotearoa New Zealand, Epidemics, Volume 41, 2022, 100657.

[9] Won M, Marques-Pita M, Louro C, Gonçalves-Sá J. Early and real-time detection of seasonal influenza onset. PLoS computational biology. 2017 Feb 3;13(2):e1005330.

[10] Dalziel BD, Bjørnstad ON, van Panhuis WG, Burke DS, Metcalf CJ, Grenfell BT. Persistent chaos of measles epidemics in the prevaccination United States caused by a small change in seasonal transmission patterns. PLoS computational biology. 2016 Feb 4;12(2):e1004655.

[11] Baker RE, Park SW, Yang W, Vecchi GA, Metcalf CJE, Grenfell BT. The impact of COVID-19 nonpharmaceutical interventions on the future dynamics of endemic infections. Proc Natl Acad Sci USA 2020; 117: 30547–53.

[12] Messacar K, Baker RE, Park SW, Nguyen-Tran H, Cataldi JR, Grenfell B. Preparing for uncertainty: endemic paediatric viral illnesses after COVID-19 pandemic disruption. The Lancet. 2022 Nov 12;400(10364):1663-5.

[13] Krauland MG, Galloway DD, Raviotta JM, Zimmerman RK, Roberts MS. Impact of Low Rates of Influenza on Next-Season Influenza Infections. Am J Prev Med. 62(4):503-510 (2002).

[14] Hamid S, Winn A, Parikh R, et al. Seasonality of Respiratory Syncytial Virus — United States, 2017–2023. MMWR Morb Mortal Wkly Rep 2023;72:355–361.

[15] Alahakoon P, McCaw JM, Taylor PG. Improving estimates of waning immunity rates in stochastic SIRS models with a hierarchical framework. Infectious Disease Modelling. 2023 Dec 1;8(4):1127-37.

[16] Public Health Agency of Canada, FluWatch, https://www.canada.ca/en/public-health/services/diseases/flu-influenza/influenza-surveillance.html, 2024

[17] Center for Disease Control and Prevention. Fluview, https://www.cdc.gov/flu/weekly/index.htm, 2024